JTTEE5 6:145-149

Low-Pressure Plasma-Sprayed (LPPS) Bioceramic Coatings with Improved Adhesion Strength and Resorption Resistance

R.B. Heimann and T.A. Vu

Prespray annealing of commercially available hydroxyapatite (HAp) plasma-spray powder at 1300 °C for 1 h in air leads to substantial densification without noticeable thermal decomposition. The resulting HAp coatings, low-pressure plasma sprayed onto Ti-6Al-4V substrates, show a dense microstructure, improved adhesion strength, and higher resorption resistance when treated for 7 days in simulated body fluid (Hank's balanced salt solution).

Keywords adhesion strength, hydroxyapatite coatings, low-pressure plasma spraying, resorption resistance, spray powder densification

1. Introduction

BIOCERAMIC COATINGS based on hydroxyapatite (HAp) are routinely applied to the shafts of titanium alloy hip endoprosthetic implants by thermal spray methods, most notably atmospheric plasma spraying (APS). To obtain bioactive coatings with controlled porosity, fracture toughness, and cohesive and adhesive strengths, and with sufficient resorption resistance, their chemical purity, phase composition, and crystallinity must be carefully optimized. Since HAp melts incongruently (Ref 1), the high temperature present in a plasma jet inevitably leads to thermal transformation into other calcium phosphates—for example, tricalcium phosphate (TCP), tetracalcium phosphate (tetrCP), or even nonbiocompatible calcia (CaO). The *in vivo* stability of coatings is strongly affected by the presence of these transformation products (Ref 2).

To improve the adhesion of the coating to the substrate, the degree of melting of the HAp particles must also be improved by an increase of the plasma enthalpy (Ref 3). High enthalpies, on the other hand, lead to increased thermal decomposition and hence to a decrease of the resorption resistance (i.e., the longevity of the coating *in vivo*). As a consequence, the plasma spray parameters and in turn the microstructure of the deposited coatings must be optimized by controlling the heat transfer from the hot core of the plasma jet to the center of the powder particle. This paper deals with the characterization of the properties of various low-pressure plasma-sprayed (LPPS) coatings produced from as-received and presintered HAp powders as well as the influence of the variation of selected plasma spray parameters on the adhesive strength of such coatings.

2. Materials and Methods

Plasma-sprayed HAp coatings were produced both from as-received AMDRY 6021 powder (Sulzer Metco Deutschland GmbH; powder P1) and powder presintered at 1300 °C for 1 h (powder P2) (Ref 4). Coatings C1, from the porous original powder P1, and coatings C2, from the presintered densified powder P2, were plasma sprayed (A 3000, Plasma-Technik AG, Wohlen, Switzerland) onto Ti-6Al-4V substrates (50 by 20 by 2 mm^3) using the set of plasma spray parameters shown in Table 1. These parameters were optimized for a maximum degree of melting of the powder particles as ascertained by a "wipe" test (Ref 5) and for maximum adhesion strength and resorption resistance of the resulting coatings. In addition, a coating C3 was deposited using powder P2 at a plasma power of 25 kW, and a coating C4 using powder P1 at a plasma power of 34 kW.

The coatings were characterized by conventional x-ray powder diffraction (XRD), laser-Raman spectroscopy (LRS), and transmission electron microscopy (TEM) in conjunction with selected-area electron diffraction (SAD) for their phase content, phase purity, and crystallinity. Scanning electron microscopy (SEM) in conjunction with energy-dispersive x-ray analysis (EDX) was used to determine the porosity of the coatings, the degree of melting of the powder particles produced by the wipe tests, as well as the thermal decomposition of HAp. The adhesion strength was estimated by the European standard tensile adhesion test procedure EN 582:1993 using adhesive DP 460 (3M Deutschland). The *in vitro* resorption resistance was assessed by characterization of coatings after immersion into simulated body fluid (Hank's balanced salt solution, or HBSS; Table 2) at 37 ± 0.5 °C for 1 and 7 days.

3. Results and Discussion

Figure 1(a) shows a TEM micrograph of the interface between the titanium alloy substrate (left bottom corner) and the

Table 1 Optimized plasma spray parameters

Plasma power, kW	30 (50 V, 600 A)
Plasma gas flow rate, L/min	30 (argon) + 4 (hydrogen)
Powder carrier gas flow rate, L/min	3 (argon)
Powder feed rate, g/min	12
Chamber pressure, mbar	60
Standoff distance, mm	220
Substrate preheating	None

R.B. Heimann and **T.A. Vu,** Department of Mineralogy, Freiberg University of Mining and Technology, Brennhausgasse 14, D 09599 Freiberg, Germany.

HAp coating (C2). Adjacent to the substrate is a thin, electron-transparent layer (am). Its existence can be attributed to extremely rapid quenching of the molten HAp particles impinging at the substrate surface, rendering the material amorphous (Ref 4). The thermal conductivity of titanium exceeds that of HAp considerably so that the latter solidifies at a rate of 10^6 to 10^7 K/s (Ref 7). The amorphous layer acts as a thermal barrier to subsequently deposited lamellae of HAp and hence promotes their crystallization due to slower cooling because of impeded heat transfer. The crystallites present in the coating are of variable size (Fig. 1b), ranging from 2 to 1000 nm, and show electron diffraction patterns consistent with that of pure HAp. On the other hand, laser-Raman spectra of plasma-sprayed HAp coatings show a strong reduction of the intensity or even a complete absence of the Raman band at 3575 cm^{-1} associated with the stretching vibration of the OH group of the HAp structure (Ref 4). This is consistent with the notion that during plasma spraying HAp loses OH groups and transforms to oxyhydroxyapatite (OHAp) or even OH-free oxyapatite (OAp). Hydroxyapatite and its derivatives are indistinguishable by XRD (Ref 8). Furthermore, a shoulder at 950 cm^{-1} was found (Ref 4) that has been attributed to amorphous HAp (Ref 9).

Table 2 Composition of HBSS in 1 L deionized water

Salt	Content, mg
NaCl	8000
$MgSO_4$	1000
KCl	400
$CaCl_2$	140
$MgCl_2$	100
Na_2HPO_4	60
KH_2PO_4	60

Source: Ref 6

Determination of the Ca/P ratio by EDX revealed that the amorphous phase has a much lower Ca/P ratio (1.15) compared to that of the crystalline HAp (1.65), which is very close to the value for stoichiometric HAp (1.67). A plausible explanation for this behavior is not yet available. Since the amorphous phase as well as very small HAp crystals and decomposition products tend to dissolve quickly in body fluid, improved resorption resistance could be obtained by postspray annealing at 900 °C for 10 h. Indeed, after this thermal treatment only HAp could be de-

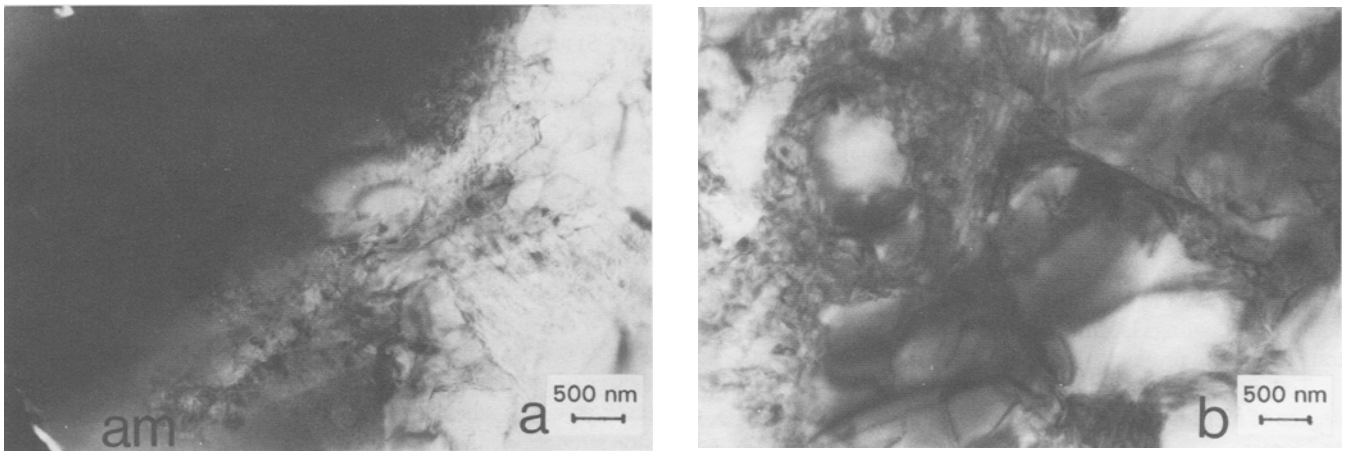

Fig. 1 TEM micrographs. (a) Amorphous calcium phosphate layer (am) adjacent to the titanium alloy substrate/coating interface. (b) Aggregate of larger and small HAp crystallites

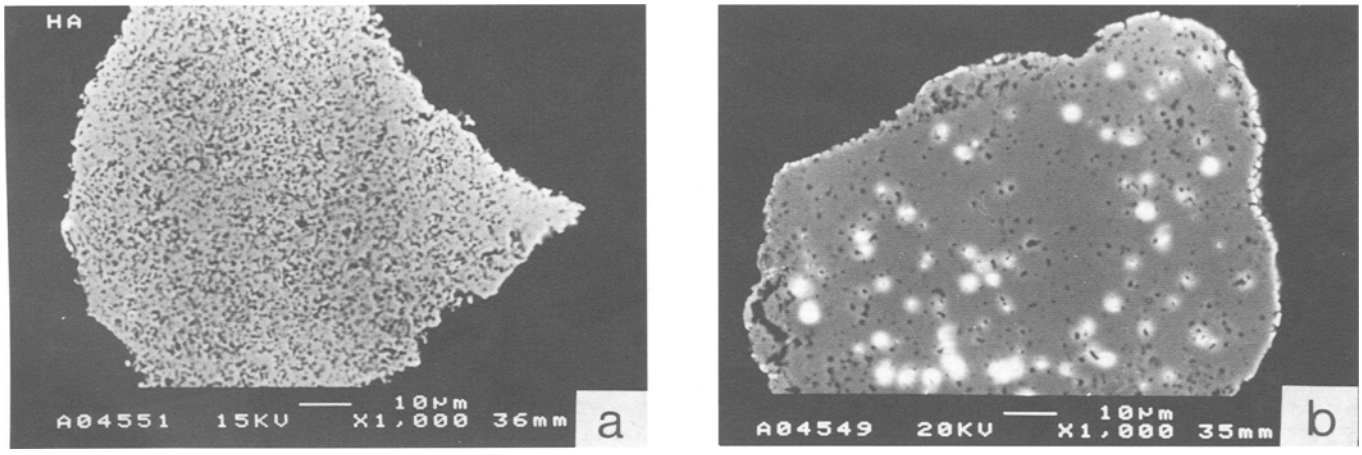

Fig. 2 SEM micrographs of polished cross-sections. (a) As-received AMDRY 6021 HAp powder (P1). (b) The same powder sintered at 1300 °C for 1 h (P2)

tected (Fig. 5c). Sintering at temperatures above 900 °C is known to increase the crystallinity of plasma-sprayed HAp coatings, with concurrent complete removal of the amorphous phase and recrystallization of the small HAp crystals (Ref 10). However, mechanical degradation of HAp coatings heat treated at 950 °C for up to 24 h was observed and attributed to the formation of tetrCP (Ref 11). This finding is at variance with results obtained recently (Ref 12) that showed, by ^{31}P-MAS-NMR spectroscopy, no formation of tetrCP during annealing of plasma-sprayed HAp coatings at 900 °C for 3 h. In fact, annealing at temperatures as low as 800 °C in air seem sufficient to restore the HAp structure within 2 h. Since the annealing experiments were performed at a low partial vapor pressure of water, the calcium phosphate structurally restored may have been OHAp or OAp. Additional ^{1}H-MAS-NMR (Ref 3) data are needed to clarify this contentious point.

The densification of the powder particles during presintering is shown in Fig. 2. Figure 2(a) shows an SEM micrograph of a polished cross section of an as-received HAp particle (P1) with a high proportion of very fine pores. Sintering at 1000 °C for 1 h does not change the appearance of the powder, whereas sintering at 1300 °C for 1 h (P2) leads to noticeable densification (Fig. 2b). Consequently, the coatings produced from powder P1 at a plasma power of 30 kW shows a high degree of porosity manifested in many highly porous zones within the coating (Fig. 3a). An increase of the plasma power to 34 kW does not lead to improvement. On the other hand, coatings produced from the presintered powder P2 do not show high porosity but rather a well-developed, dense microstructure (Fig. 3b). This holds true for coatings produced from powder P2 at a lower plasma power of 25 kW (C3).

These findings are supported by the results of the wipe tests. A glass slide was moved quickly through the plasma jet, and hence the morphology and rheology of individually solidified particles could be studied. Figure 4(a) shows a particle of the as-received powder P1; the high degree of unmelted material attests to a severely restricted heat transfer from the surface of the particle to its core. Figure 4(b), on the other hand, displays a well-molten particle "pancake" splat of the type that is likely to produce a dense and homogeneous coating with improved heat

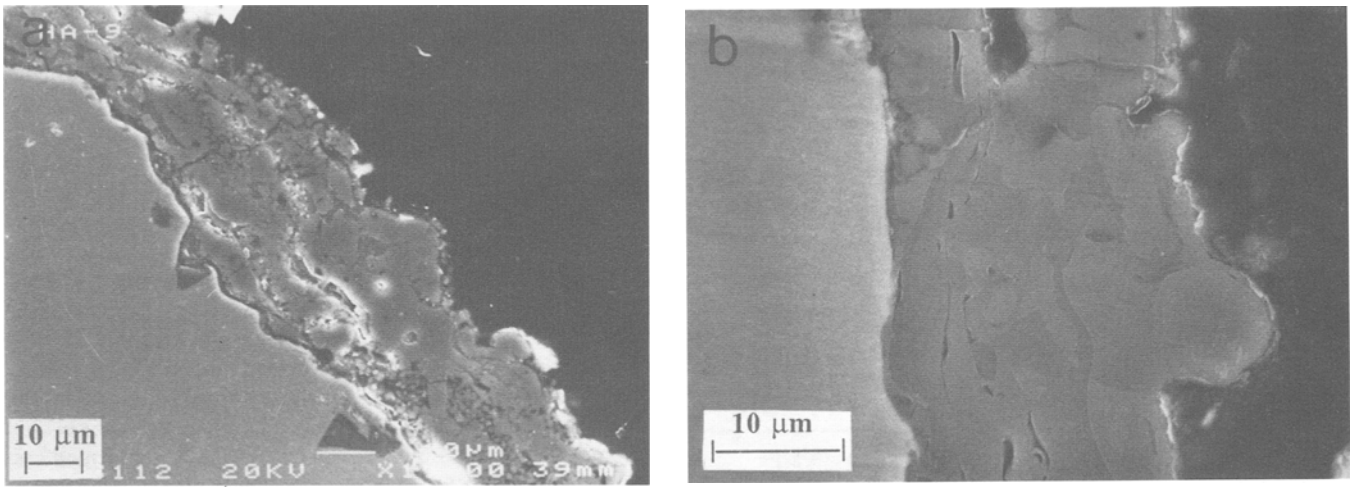

Fig. 3 SEM micrographs of polished cross-sections of HAp coatings. (a) Produced from as-received powder P1, 30 kW (C1). (b) Produced from presintered powder P2, 30 kW (C2)

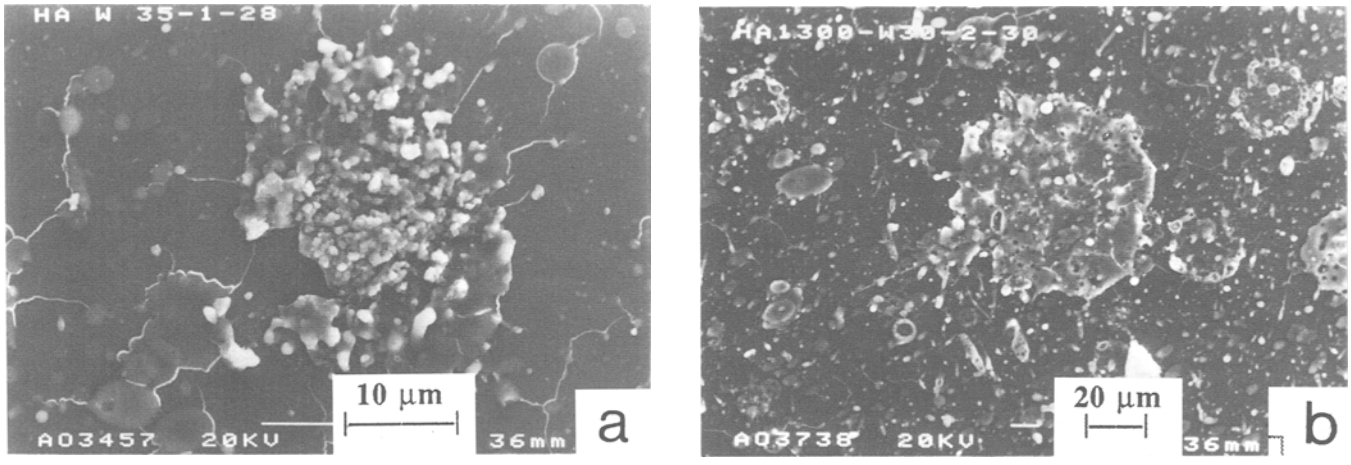

Fig. 4 Wipe tests at a plasma power of 30 kW of as-received powder P1 (a) and presintered powder P2 (b) at standoff distances between 280 and 300 mm

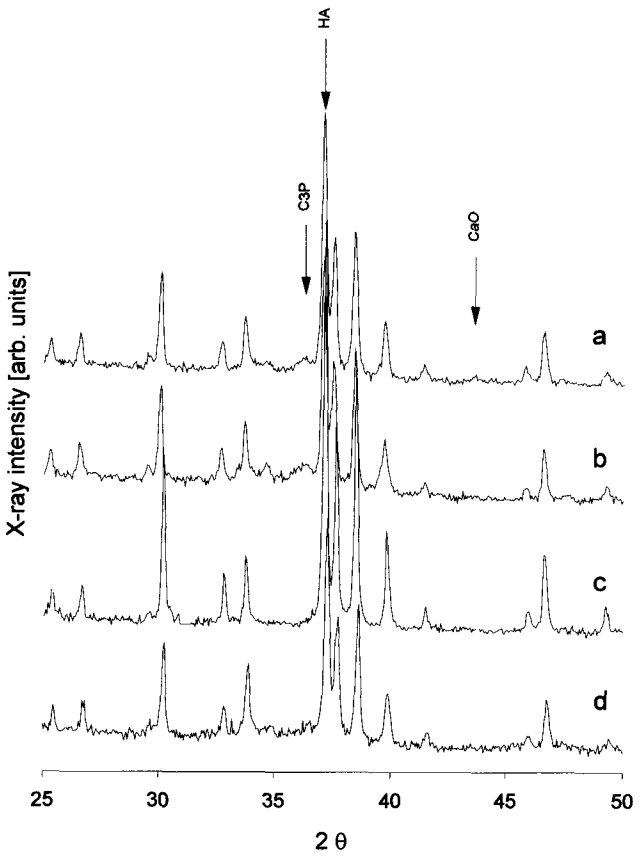

Fig. 5 X-ray diffractograms of coatings C1 (a), C2 (b), C2 postspray annealed at 900 °C for 10 h (c), and C3 (d)

Table 3 Tensile adhesion strength (EN 582:1993) of coatings C1 and C2 as a function of immersion time in HBSS (n = 5)

Immersion time, days	Adhesion strength, MPa	
	Coating C1	Coating C2
0	20.5 ± 0.9	29.5 ± 2.1
1	13.1 ± 0.8	23.4 ± 1.1
7	10.4 ± 1.6	24.0 ± 1.8

transfer, leading to increased cohesive and adhesive strengths. Improved heat transfer may also permit the development of a diffusive bonding mode beyond a merely mechanical interlocking of the splats with the roughened substrate surface. Line scan analyses by STEM-EDX showed that a thin interdiffusion zone (about 70 nm) exists between the substrate and coating, where titanium atoms have diffused into the coating and calcium, phosphorus, and oxygen atoms into the titanium substrate (Ref 4). This conclusion was also confirmed by Auger electron spectroscopy (Ref 13). Reports in the literature that reactively formed calcium titanate phases such as $CaTiO_3$ (perovskite) (Ref 14) or $CaTi_2O_5$ (Ref 15) could act as chemical bonding agents support the notion of a limited interfacial diffusion.

Tensile adhesion strength tests performed on coatings C1 and C2 (n = 5) showed that presintering of the powder improves adhesion strength. Table 3 shows increased adhesion strength for the as-sprayed coating C2 compared to coating C1. On the other hand, adhesion strength for both coatings decreases with increased immersion time in HBSS. It should be noted, however, that the coatings C2 produced from presintered powder P2 under the conditions shown in Table 1 retain, even after 7 days in HBSS, a considerable adhesion strength of around 25 MPa—more than twice the value found for coatings C1 treated under identical conditions. No deterioration of the microstructure of the coatings after immersion could be detected by SEM.

X-ray diffraction studies were performed to obtain information on the thermal decomposition of HAp during plasma spraying. Figure 5 shows XRD spectra of coatings C1, C2, and C3 as well as a coating C2 sintered at 900 °C for 10 h. Coatings C1 and C2 both contain traces of TCP; in addition, coating C1 contains small amounts of CaO. Since C2 was produced from the presintered densified powder P2, the absence of even traces of CaO in the coating may be attributed to the optimized heat transfer (compare Fig. 5b and 5a). Likewise, a reduction of the plasma power from 30 kW to 25 kW results in a noticeable decrease of the decomposition product TCP (compare Fig. 5b and 5d).

4. Conclusions

The properties of adhesion strength and resorption resistance of plasma-sprayed HAp coatings depend on the spray parameters and to a large extent on the microstructure of the powder particles. Since the micropores in the as-received HAp powder strongly influence the heat transfer from the plasma jet through the particle surface into the core, the particles melt only partially during their short residence time in the jet. Thermal treatment of the powder before plasma spraying at a temperature of 1300 °C for 1 h leads to powder densification, which increases the heat transfer during plasma spraying and thus the degree of melting of the particles at substantially reduced plasma power. Consequently, the coating properties can be improved toward higher tensile adhesion strength to the substrate and also higher *in vitro* resorption resistance. Since presintering can be performed easily and economically, it may be preferred over densification of powder particles using flame, plasma, or high-velocity oxyfuel spraying techniques as suggested elsewhere (Ref 16). The importance in terms of the adhesion of chemical processes occurring at the substrate/coating interface is noted.

Acknowledgments

We gratefully acknowledge support of this work by a research grant of the State Ministry of Science and the Arts of the Free State of Saxony (grant No. 4-7541.82-0390/414). Thanks are due to Professor Bernhard Wielage of Technical University Chemnitz-Zwickau, who kindly provided access to the LPPS equipment.

References

1. K. deGroot, Medical Applications of Calcium Phosphate Bioceramics, *J. Ceram. Soc. Jpn.*, Vol 99, 1991, p 917-926
2. C.P.A.T. Klein, P. Patka, J.G.C. Wolke, J.M.A. de Blieck-Hogervorst, and K. deGroot, Long-Term *in vivo* Study of Plasma-sprayed Coatings on Titanium Alloys of Tetracalcium Phosphate, Hydroxyapatite and alpha-Tricalcium Phosphate, *Biomaterials*, Vol 15, 1994, p 146-150

3. R. McPherson, N. Gane, and T.J. Bastow, Structural Characterization of Plasma-Sprayed Hydroxylapatite Coatings, *J. Mater. Sci. Mater. Med.*, Vol 6, 1995, p 327-334
4. T.A. Vu and R.B. Heimann, Improvement of the Adhesion Strength of Plasma-Sprayed Bioceramic Coatings, *DVS-Berichte*, Vol 175, 1996, p 178-181
5. H. Gruner, Vacuum Plasma Spray Quality Control, *Thin Solid Films*, Vol 118, 1984, p 409-420
6. O. Ohtsuka, M. Matsura, N. Chida, M. Yoshinori, T. Sumii, and T. Derand, Formation of Hydroxyapatite on Pure Titanium Substrates by Ion Beam Dynamic Mixing, *Surf. Coat. Technol.*, Vol 65, 1994, p 224-230
7. J.M. Houben, "Relation of the Adhesion of Plasma Sprayed Coatings to the Process Parameters Size, Velocity and Heat Content of the Spray Particles," Ph.D. thesis, Technical University Eindhoven, Eindhoven, The Netherlands, 1988
8. H. Keller, "Biokompatible Werkstoffe: Herstellung und Charakterisierung von Plasmagespritzten Hydroxylapatitschichten auf Femurschäften von Titan-Hüft-Prothesen," doctoral thesis, Universität Tübingen, Tübingen, Germany, 1992
9. M. Weinlaender, J. Beumer III, E.B. Kenny, P.K. Moy, and F. Adar, Raman Microprobe Investigations of Calcium Phosphate Phases of Three Commercially Available Plasma-Flame-Sprayed Hydroxyapatite-Coated Dental Implants, *J. Mater. Sci. Mater. Med.*, Vol 3, 1992, p 397-401
10. M.J. Filiaggi, N.A. Coombs, and R.M. Pilliar, Characterization of the Interface in the Plasma-Sprayed HA Coating/Ti-6Al-4V Implant System, *J. Biomed. Mater. Res.*, Vol 25, 1991, p 1211-1229
11. F. Brossa, A. Cigada, R. Chiesa, L. Paracchine, and C. Consonni, Post-Deposition Treatment Effects on Hydroxyapatite Vacuum Plasma Spray Coatings, *J. Mater. Sci. Mater. Med.*, Vol 5, 1994, p 855-857
12. J. Vogel, C. Rüssel, G. Günther, P. Hartmann, F. Vizethum, and N. Bergner, Characterization of Plasma-Sprayed Hydroxyapatite by ^{31}P-MAS-NMR and the Effect of Subsequent Annealing, *J. Mater. Sci. Mater. Med.*, Vol 7, 1996, p 495-499
13. R.B. Heimann, T.A. Vu, and M.L. Wayman, Bioceramic Coatings: State-of-the-Art and Recent Development Trends, *Eur. J. Miner.*, in press
14. K. deGroot, R.T.G. Geesink, C.P.A.T. Klein, and P. Serekian, Plasma Sprayed Coatings of Hydroxylapatite, *J. Biomed. Mater. Res.*, Vol 21, 1987, p 1375-1381
15. H. Ji, C.B. Ponton, and P.M. Marquis, Microstructural Characterization of Hydroxylapatite Coatings on Titanium, *J. Mater. Sci. Mater. Med.*, Vol 3, 1992, p 283-287
16. P. Cheang and K.A. Khor, Bioceramic Powder and Coatings by Thermal Spray Techniques, *Thermal Spraying—Current Status and Future Trends*, A. Ohmori, Ed., High Temperature Society of Japan, Osaka, 1995, p 181-186